Supplementary Information

Modular Functionalization of Crystalline Graphene by Recombinant Proteins: A Nanoplatform for Probing Biomolecules

Abhishek Tyagi,[1] Xiaotian Liu,[1] Irfan Haider Abidi,[1] Zhaoli Gao, [1,2] Byung Min Park,[1] Xiangze Zeng,[3] Xuewu Ou,[1] Aldrine Abenoja Cagang,[1] Minghao Zhuang,[1] Md Delowar Hossain,[1] Kai Zhang,[6] Lu-Tao Weng,[1,4*] Fei Sun[1,5*] and Zhengtang Luo[1*]

[1] Department of Chemical and Biological Engineering, The Hong Kong University of Science and Technology, Hong Kong

[2] Department of Physics and Astronomy, Department of Materials Science and Engineering, University of Pennsylvania, Philadelphia, Pennsylvania 19104, United States of America

[3] Department of Chemistry, The Hong Kong University of Science and Technology, Hong Kong

[4] Materials Characterization and Preparation Facility, The Hong Kong University of Science and Technology, Hong Kong

[5] Center of Systems Biology and Human Health, School of Science and Institute for Advanced Study, The Hong Kong University of Science and Technology, Hong Kong

[6] School of Electro-mechanical Engineering, Guangdong University of Technology, Guangzhou, China

The protein sequences for the proteins we have used as follows:

a). AAA amino acids (SpyTag-ELP-SpyTag-ELP): 225; Molecular weight: 20777.1 Da

MKGSSHHHHHHVDAHIVMVDAYKPTKLDGHGVGVPGVGVPGVGVPGEGVPGVGVPG
VGVPGVGVPGVGVPGEGVPGVGVPGVGVPGVGVPGVGVPGEGVPGVGVPGVGELAHI
VMVDAYKPTKTSVPGVGVPGVGVPGEGVPGVGVPGVGVPGVGVPGEGVPGV
GVPGVGVPGVGVPGVGVPGEGVPGVGVPGVGVPGGLLDAHIVMVDAYKPTK LEWKK

b). BYB (Spycatcher-cpYFP-Spycatcher) amino acids: 488; Molecular weight: 53377.3 Da

MAMVDTLSGLSSEQGQSGDMTIEEDSATHIKFSKRDEDGKELAGATMELRDSSGKTIST
WISDGQVKDFYLYPGKYTFVETAAPDGYEVATAITFTVNEQGQVTVNGKATKGDAEL
MYNSDNVYIMADKQKNGIKANFKIRHNVEDGSVQLADHYQQNTPIGDGPVLLPDNHYL
SFQSVLSKDPNEKRDHMVLLEFVTAAGITLGMDELYNVDGGSGGTGSKGEELFTGVVPI
LVELDGDVNGHKFSVSGEGEGDATYGKLTLKLICTTGKLPVPWPTLVTTLGYGLKCFAR
YPDHMKQHDFFKSAMPEGYVQERTIFFKDDGNYKTRAEVKFEGDTLVNRIELKGIGFKE
DGNILGHKLEYNGSAMVDTLSGLSSEQGQSGDMTIEEDSATHIKFSKRDEDGKELAGAT
MELRDSSGKTISTWISDGQVKDFYLYPGKYTFVETAAPDGYEVATAITFTVNEQGQVTV
NGKATKGDAHILEHHHHHH

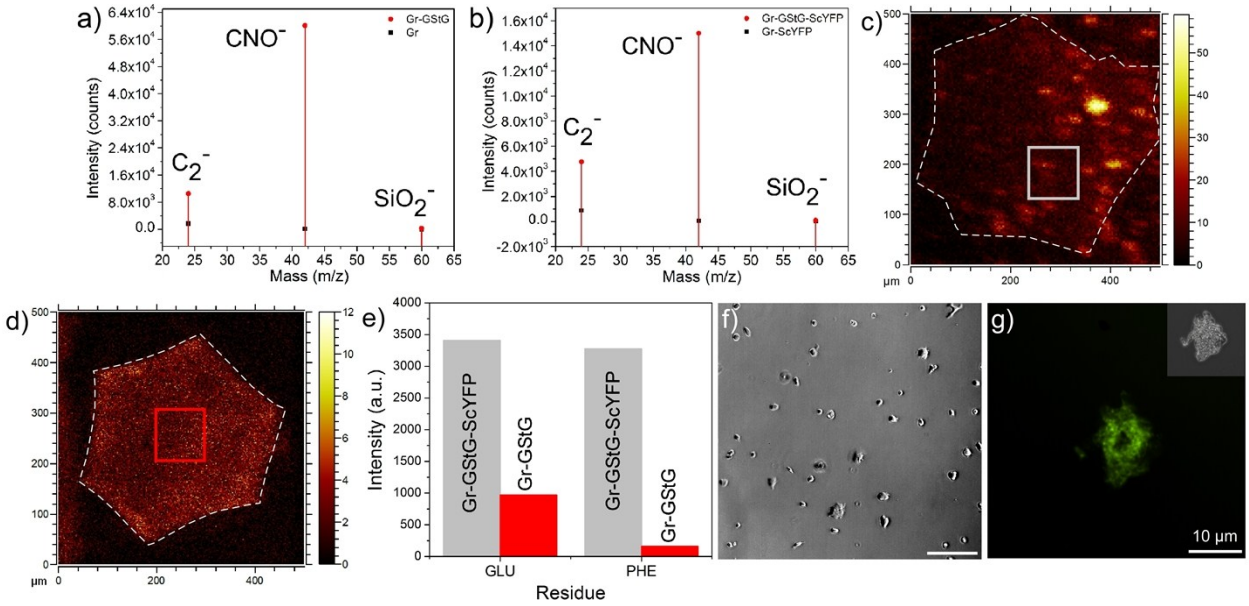

Figure S1: ToF-SIMS intensities for chemical imaging. Intensities of SiO_2^-, C_2^-, CNO^-, and $C_2H_3O_2^-$ for a) GStG on graphene, and b) ScYFP on Gr-GStG. SpyCatcher binds to SpyTag confirmed by ToF-SIMS mapping for selective region for Glu (E) and Phe (F) marked in gray and red colour; c) on Gr-GStG-ScYFP surface and d) on Gr-GStG surface. e) Intensities count for Glu and Phe on Gr-GStG-ScYFP and Gr-GStG surface. f) MCF7 cells on glass substrate surfaces, the Scale bar are 10 µm. g) Fluorescence microscopy for Gr-GStG-ScYFP complex on 3D graphene foam, inset bright field image for 3D graphene foam.

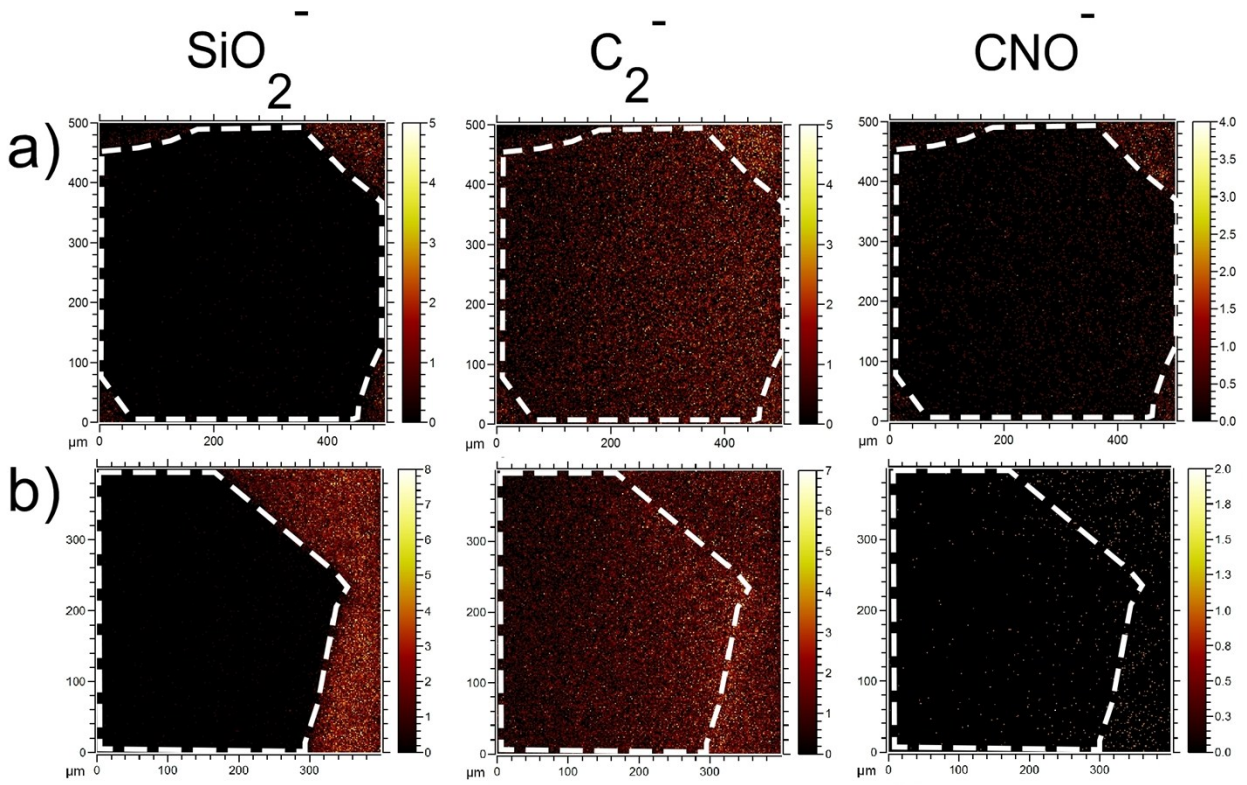

Figure S2: ToF-SIMS analysis for ScYFP transferred to graphene. a) Representing C_2^- ions for graphene, SiO_2^- for silicon oxide, and CNO^- ions for peptide backbone. b) When ScYFP transferred to the surface, the mapping of CNO^- ions confirms the weak interaction with SCG.

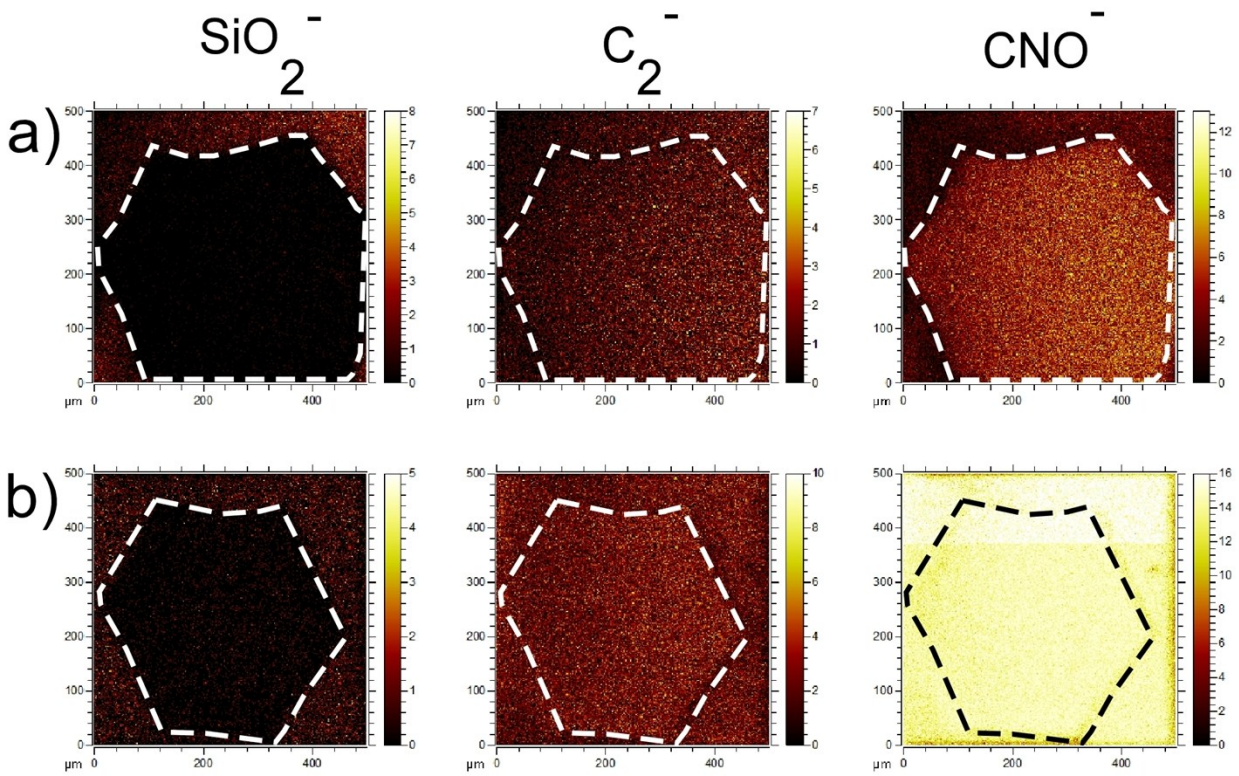

Figure S3: ToF-SIMS analysis for protein on graphene. ToF-SIMS mapping shows C_2^- ions for graphene, SiO_2^- for silicon oxide, and CNO^- ions for peptide backbone. a) BSA (100 nM) on SCG, and b) Skim milk (5 % w/v) on SCG.

Supplementary Note 1. Morphology of GStG on graphene surface by AFM

After the disposition, as shown in Figure 3b, we observed that the thickness of GStG has an average height of ~2-3 nm decorated throughout the graphene surface (see height profile on Figure 3d). After further functionalization with SpyCatcher, surface coverage of protein has significantly increased from ~2-3 to 5-6 nm, with a height raise of 3-4 nm, as shown in Figure S3c and height profile in Figure S3d. To further confirm the morphology change, we have performed the AFM measurements on various concentrations of GStG solution that were deposited on the graphene surface. As shown in the Figure S4, as the GStG concentration is increased, the morphology changes from isolated islands (Figure S4a) into network structure (Figure S4b) and then into thick film of aggregations (Figure S4c). As a control experiment, SpyTag-ELP-SpyTag-ELP protein (AAA protein) that lacks graphene binding peptides was found to be absorbed non-specifically on the whole silicon wafer, with no selectivity on graphene surface, as shown in the Figure S5a-c.

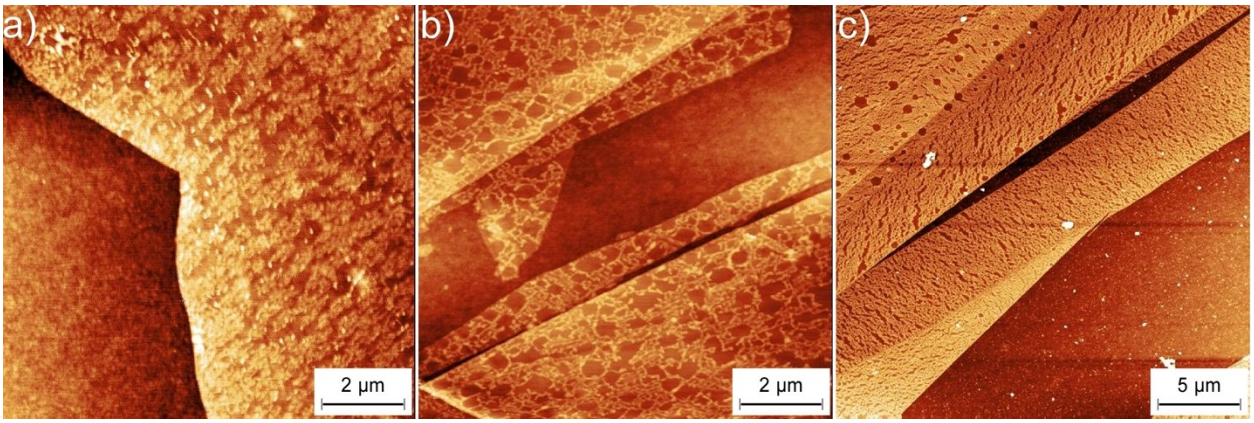

Figure S4: AFM imaging on exfoliated graphene for GStG on exfoliated graphene. a) GStG at 100 nM concentration on graphene. b) GStG at 1 µM concentration on graphene. c) GStG at 10 µM on graphene.

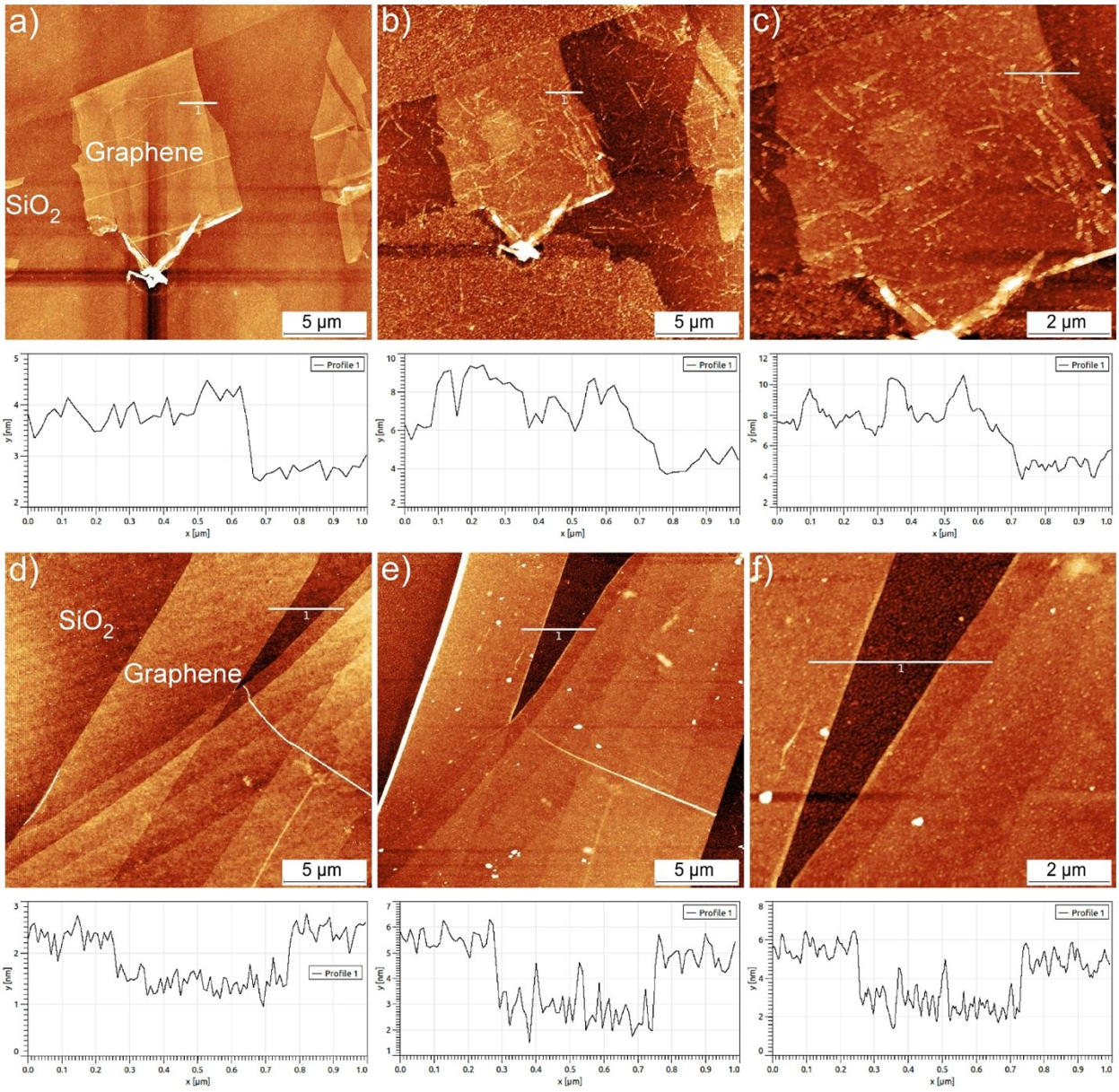

Figure S5: AFM imaging on exfoliated graphene for SpyTag and SpyCatcher. a) Exfoliated graphene sample position before AFM, the image shows the graphene is ~1 nm thick. b) and c) AAA protein on exfoliated graphene, the thickness increases ~2-2.5 nm. d) Exfoliated graphene before transferring ScYFP. e) and f) ScYFP on exfoliated graphene, the average thickness increases to ~3 nm.

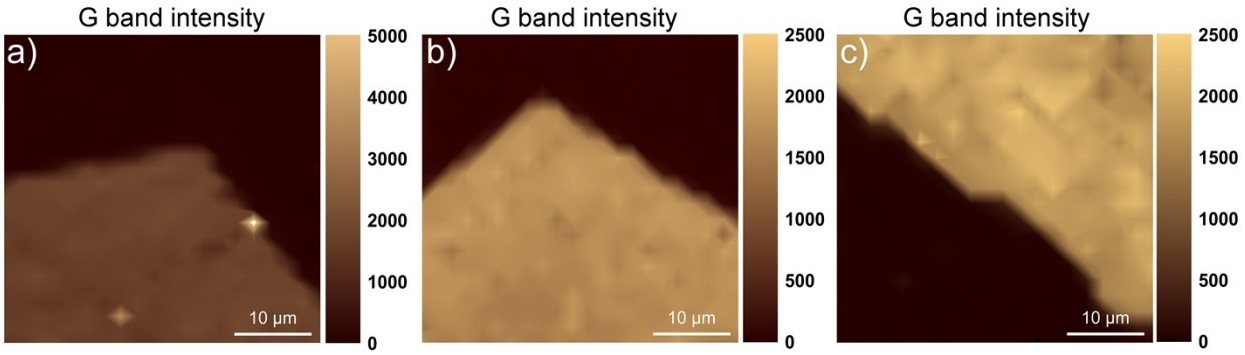

Figure S6: Surface characterization by Raman mapping. Acquired with 514.7 nm laser at the center of single crystal graphene, a) for graphene at 1586 cm^{-1}, b) after transfer of GStG on graphene at 1593 cm^{-1}, and c) after transfer of SpyCatcher-YFP on Gr-GStG unit at 1598 cm^{-1}, showing the red shift indicating functionalizing of graphene surface.

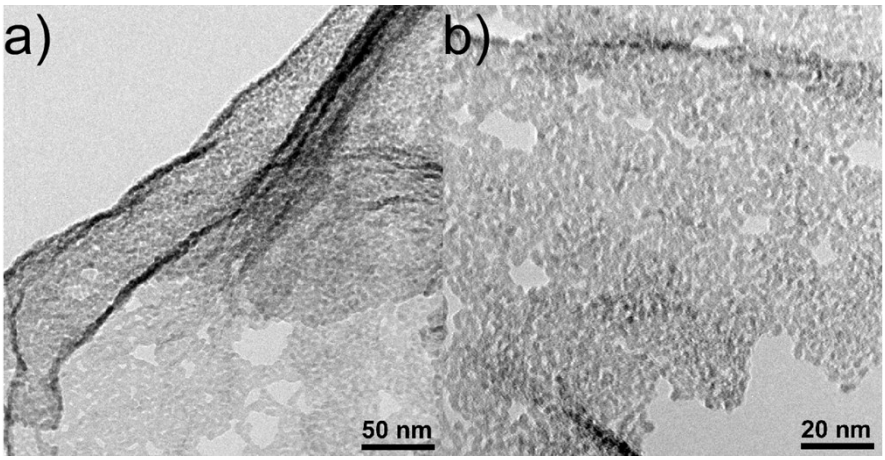

Figure S7: The Transmission electron microscopy images of GStG. The GStG was transferred on glow-discharged copper grid, the average size of GStG was 3-5 nm for a) 50 nm and b) 20 nm.

Supplementary Note 2. Molecular dynamics (MD) simulations for GStG-Graphene interactions

As explained in materials and method, six models of GStG adsorption on graphene nanosheet with respect to time scale were used in MD simulations. The whole GStG sequence was decomposed into three main parts: P1 (grey), SpyTag (red) and P2 (blue) together with a linker (black). For all six models, the distance of center of mass of GStG to graphene nanosheet surface dropped dramatically after 15 ns (Figure S9), indicating that peptide started its adsorption on graphene nanosheet within ~15 ns of production run, which is consistent with the sharp increase of the number of contact (Nc) (Figure S9). The initial and final configurations at 500 ns of GStG for each model were also shown in the inserts of Figure S9. The adsorption of GStG also caused the distortion of its 3D structure, as revealed by the change in both the distance of center mass and Nc. The number of contact Nc, after a rapid increase at the first 15 ns, gradually increased with simulation time for all six models. It reached ~150 at ~100 ns. After 100 ns a further increase was observed for all models except S9c and S9e. Although some fluctuations were observed throughout the simulations, the general trend for the remaining 4 models is that Nc gradually increased from ~150 at 100 ns to ~300 at 300 ns (see Figure S9a, b, d, f). GStG adsorption appeared to be stabilized from 300 to 500 ns and reached its thermodynamic maximum Nc of ~350. Similar trends were observed for the contact area as shown in Figure S10a: (1) within the first ~15 ns, a steep increase of contact area from 0 to over ~400 $Å^2$ for all models; and (2) after ~15 ns, the contact area gradually increased with time and at 500 ns reached ~1000 $Å^2$ for models 1, 2, 4, 6 and ~500 $Å^2$ for models 3 and 5. All these results confirm the strong adsorption of GStG on graphene nanosheet for this span of time scale. To observe the conformational change of GStG upon adsorption, we have also calculated the root mean square

deviation (RMSD) and radius of gyration (Rg) as a function of simulation time (Figure S10b and 10c). The RMSD and Rg values, show the dynamic change in peptide position and size within 500 ns. In spite of some fluctuations, the general trend for both RMSD and Rg is that they gradually increased with simulation time and stabilized at 500 ns, therefore, no need to extend simulations for further calculations. Thus, it is clear from these results that the GStG lost its 3D conformation and spread over the two-dimensional graphene nanosheet, indicating that GStG was well adsorbed on graphene nanosheet surface.

In order to investigate which residues, interact preferentially with graphene nanosheet, the van der Waals (vdW) interaction energy between each residue in GStG and graphene nanosheet has been calculated and the averaged value of each residue from 300 to 500 ns for the six models is presented in Figure S11. In order to have a global comparison among the sequences P1, SpyTag and P2, the vdW interaction energies of their residues were averaged and presented in Figure 4b for the six models. It can be observed that the average energies for P1 and P2 were ~ -9 kcal/mol, as compared to ~ -4 kcal/mol for SpyTag for most of simulations. These results demonstrate that P1 and P2 bound near to graphene nanosheet surface as opposed to SpyTag. If we took a closer look at Figure S11, we found that the residues Trp, His, and Tyr in both P1 and P2 showed higher vdW energies of <-16 kcal/mol for all models. These results suggest that these three residues played a major contribution in binding GStG to hydrophobic graphene nanosheet surface. Therefore, the MD simulations demonstrate that owing to the strong interaction between the residues Trp, His and Tyr and graphene nanosheet, GStG is present in a special configuration with P1 and P2 binding close to the graphene nanosheet surface and SpyTag hanging at the top.

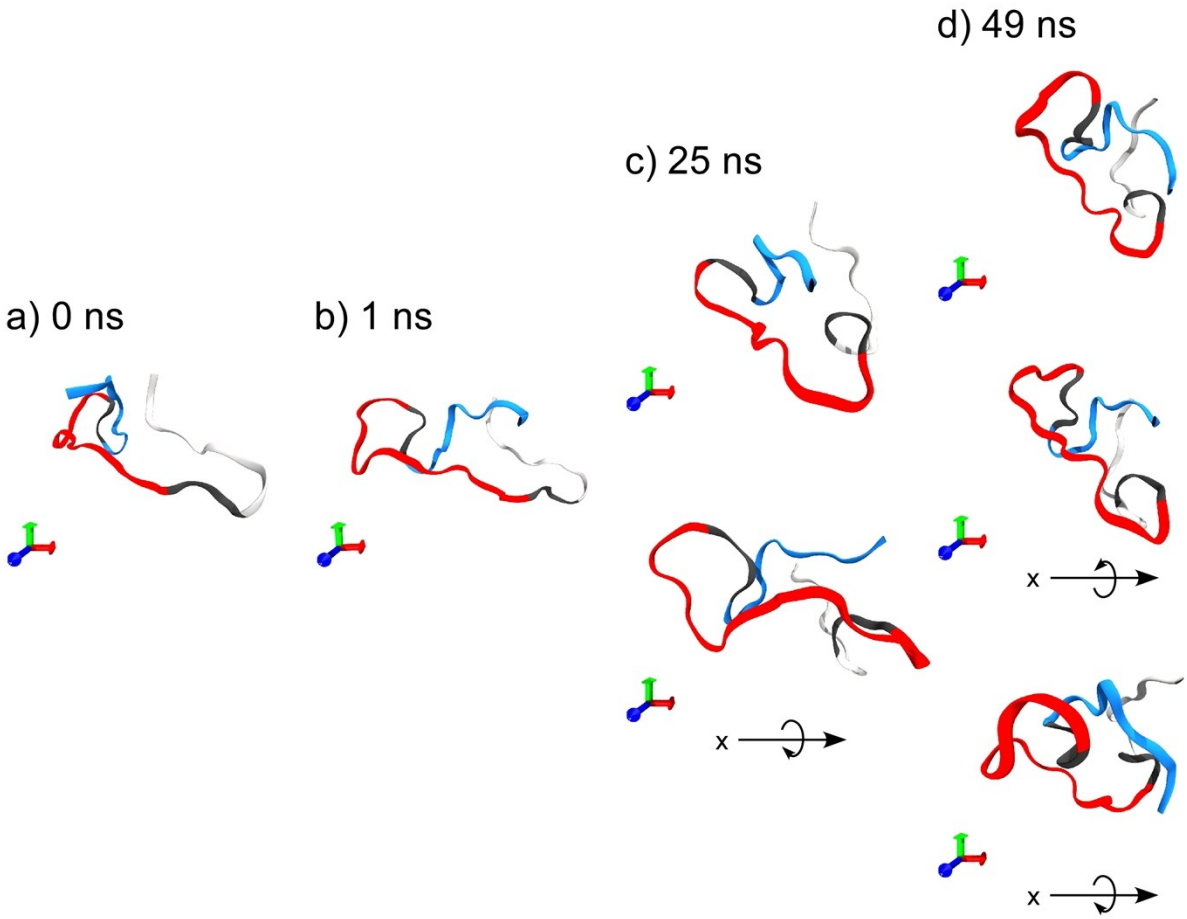

Figure S8: GStG models. Models for GStG marked as grey, red, black and blue for P1, SpyTag, Linker, and P2. a) Initial model of GStG before simulations, the model was rotated along inset axis by +45°, b) After 1 ns simulations c) after 25 ns d) After 49 ns of simulations, the model was rotated along the inset axis by -45° and +45°.

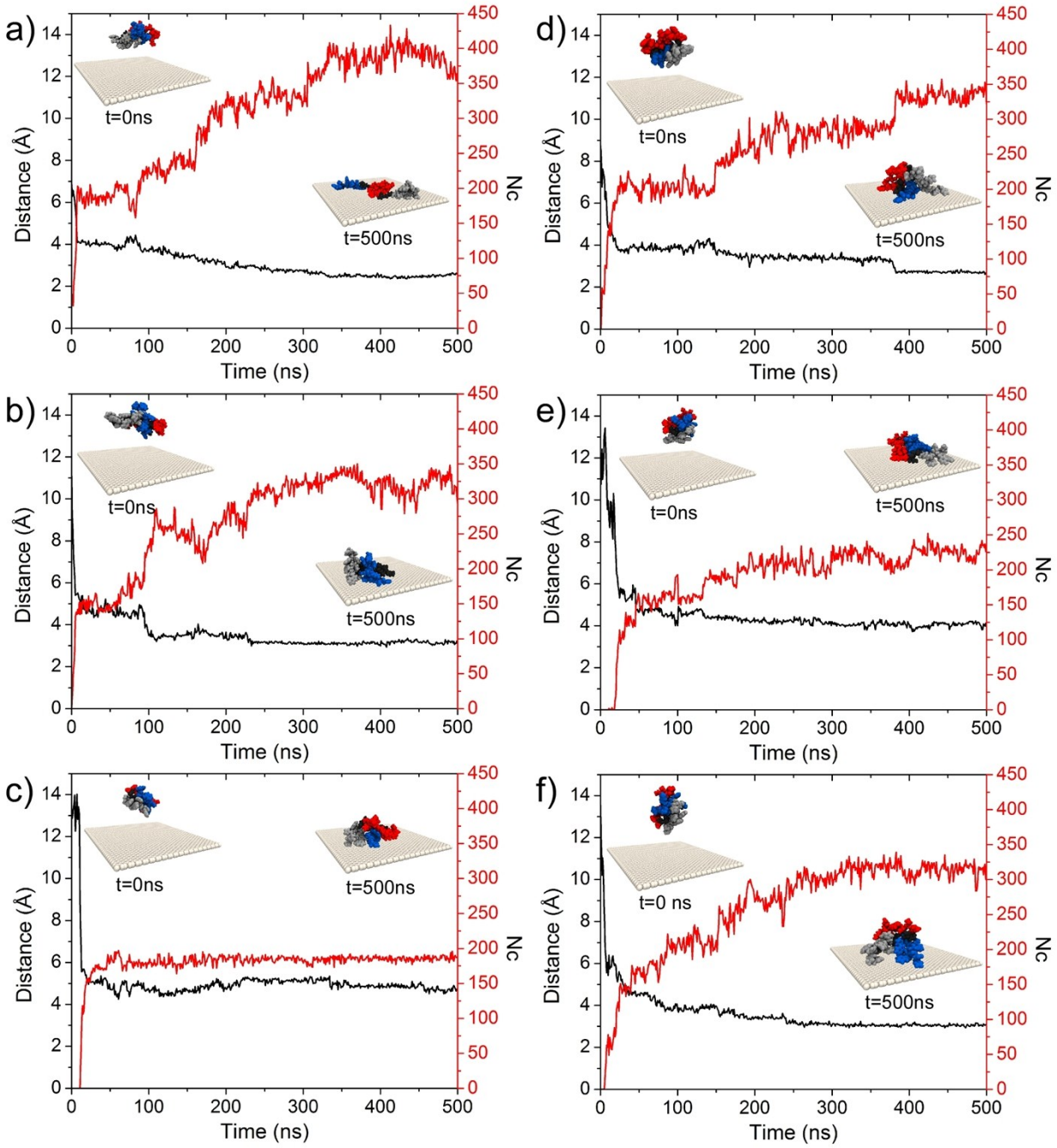

Figure S9: Adsorption dynamics calculations of GStG on graphene. Simulation calculations for GStG on graphene nanosheet interactions for contact number and distance for all models.

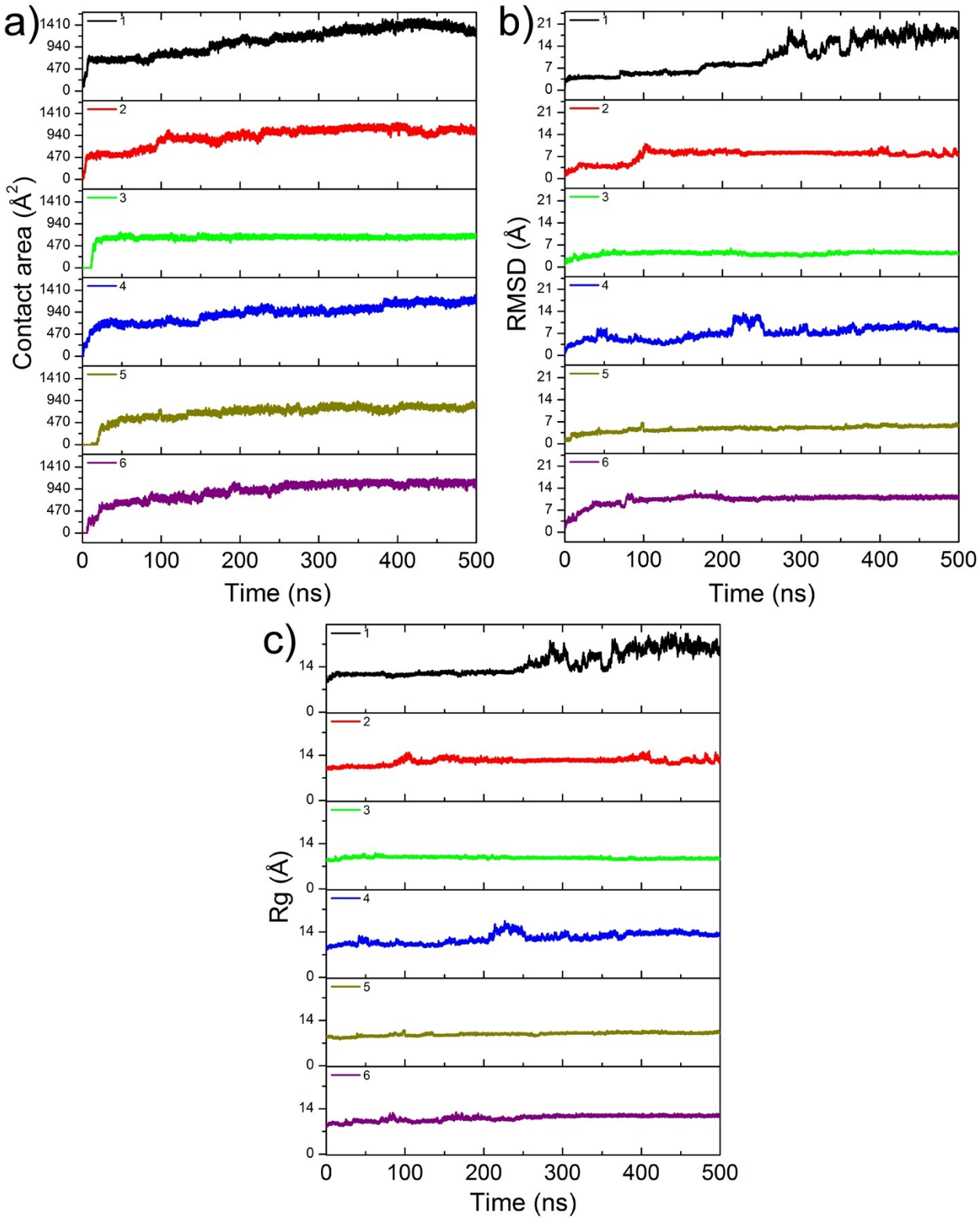

Figure S10: Conformational dynamics calculations of GStG. Simulations were performed on six models of GStG for 500ns. a) Contact area, b) Root mean square deviations (RMSD), and (c) Radius of gyration (Rg).

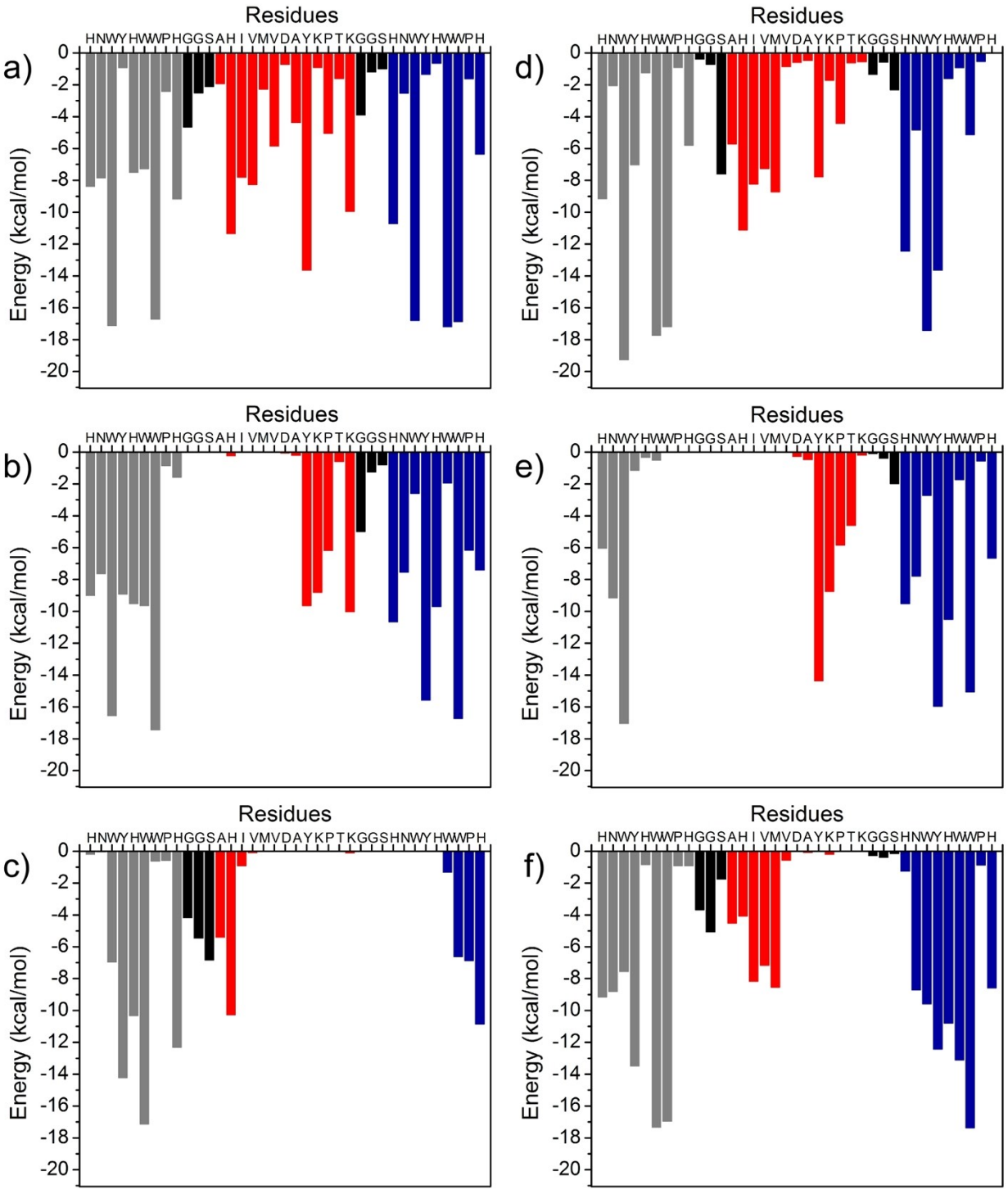

Figure S11: Interaction energy calculations for GStG adsorption on graphene. The interaction energy was calculated for six models of GStG. The calculations were performed for last 200ns (300-500ns). Interaction energy in gray, black, red and blue color for P1, Linker, SpyTag, and P2 after 500ns.

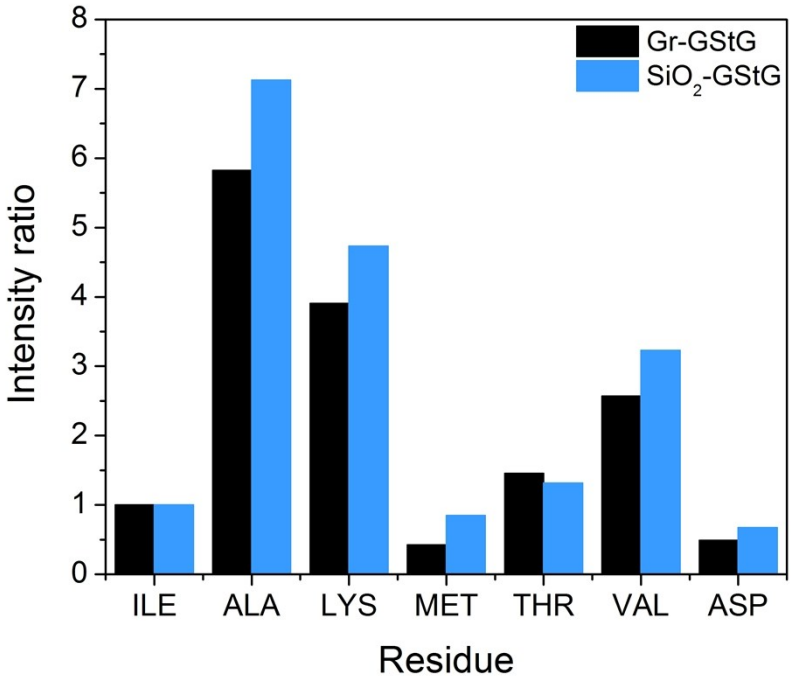

Figure S12: ToF-SIMS intensities ratios between the residues of SpyTag of GStG on SCG and SiO_2 surface with respect to the residue for Ile from SpyTag. The intensity ratio showing conformational stability of GStG on graphene and SiO_2 surface.

Amino acids	Mass (m/z)	Gr-GStG	SiO_2-GStG
GLY	30.0346	17011.78	148308.7
ILE	86.1008	3033.36	20274.58
ALA	44.0502	17662.82	144420.3
LYS	56.0493	20474.47	104531.3
SER	60.0443	4434.29	41944.24
MET	61.0088	1290.05	17189.28
THR	69.033	4420	26643
ASN	70.0297	4366.15	30907.48
PRO	70.0699	30375.81	263963.7
VAL	72.0855	7797.81	65430.41
ASP	87.0571	1485.26	13695.22
HIS	110.0807	47928.49	411119.5
TRP	130.064	13855.22	274081.5

TableS1: The ToF-SIMS intensity for GStG on SCG and SiO_2 wafer. The amino acids in GStG were listed, with their mass and positive ions intensities.